Article

Immunity

By Capturing Inflammatory Lipids Released from Dying Cells, the Receptor CD14 Induces Inflammasome-Dependent Phagocyte Hyperactivation

Graphical Abstract

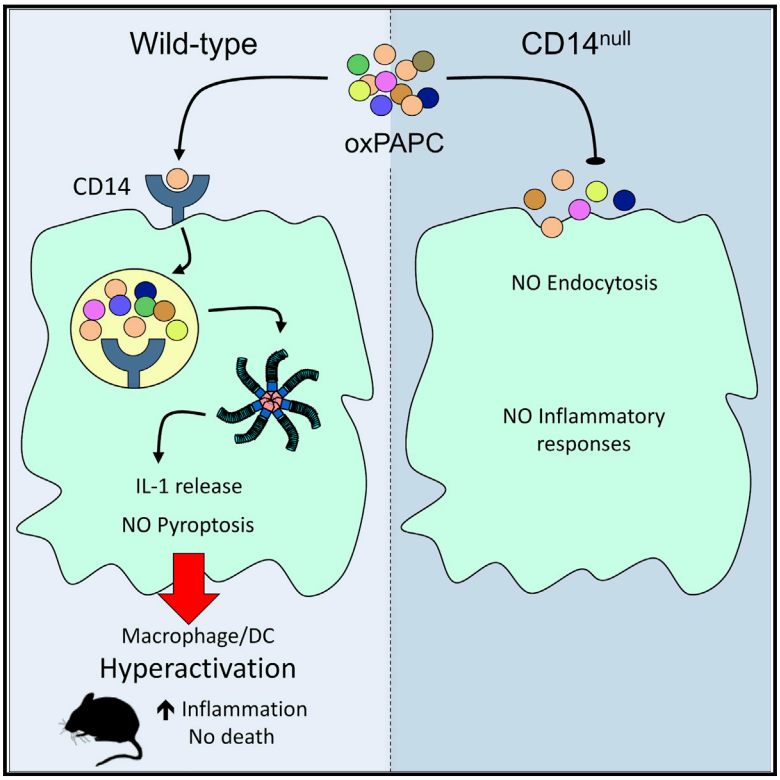

Authors

Ivan Zanoni, Yunhao Tan, Marco Di Gioia, James R. Springstead, Jonathan C. Kagan

Correspondence

ivan.zanoni@childrens.harvard.edu (I.Z.), jonathan.kagan@childrens.harvard.edu (J.C.K.)

In Brief

Inflammasomes elicit pyroptosis or cell hyperactivation, with the latter defined as living cells that release IL-1. Zanoni et al. report that CD14 captures distinct lipids within oxPAPC to promote dendritic cell and/or macrophage hyperactivation. Unlike pyroptotic stimuli, oxPAPC lipids promote long-term IL-1 release from cells and non-lethal inflammation in mice.

Highlights

- CD14 endocytosis upon oxPAPC binding prevents inflammation via TLR4
- CD14 endocytosis upon oxPAPC binding promotes inflammation via caspase-1 and -11
- oxPAPC and its components induce IL-1 release from living (hyperactive) phagocytes
- Conditions of cell hyperactivation induce non-lethal inflammatory sepsis in mice

Zanoni et al., 2017, Immunity *47*, 697–709
October 17, 2017
https://doi.org/10.1016/j.immuni.2017.09.010

CellPress

Immunity
Article

By Capturing Inflammatory Lipids Released from Dying Cells, the Receptor CD14 Induces Inflammasome-Dependent Phagocyte Hyperactivation

Ivan Zanoni,[1,2,4,*] Yunhao Tan,[1,4] Marco Di Gioia,[1,4] James R. Springstead,[3] and Jonathan C. Kagan[1,5,*]
[1]Harvard Medical School and Division of Gastroenterology, Boston Children's Hospital, Boston, MA, USA
[2]Department of Biotechnology and Biosciences, University of Milano-Bicocca, Milan, Italy
[3]Department of Chemical and Paper Engineering, Western Michigan University, Kalamazoo, MI, USA
[4]These authors contributed equally
[5]Lead Contact
*Correspondence: ivan.zanoni@childrens.harvard.edu (I.Z.), jonathan.kagan@childrens.harvard.edu (J.C.K.)
https://doi.org/10.1016/j.immuni.2017.09.010

SUMMARY

A heterogeneous mixture of lipids called oxPAPC, derived from dying cells, can hyperactivate dendritic cells (DCs) but not macrophages. Hyperactive DCs are defined by their ability to release interleukin-1 (IL-1) while maintaining cell viability, endowing these cells with potent aptitude to stimulate adaptive immunity. Herein, we found that the bacterial lipopolysaccharide receptor CD14 captured extracellular oxPAPC and delivered these lipids into the cell to promote inflammasome-dependent DC hyperactivation. Notably, we identified two specific components within the oxPAPC mixture that hyperactivated macrophages, allowing these cells to release IL-1 for several days, by a CD14-dependent process. In murine models of sepsis, conditions that promoted cell hyperactivation resulted in inflammation but not lethality. Thus, multiple phagocytes are capable of hyperactivation in response to oxPAPC, with CD14 acting as the earliest regulator in this process, serving to capture and transport these lipids to promote inflammatory cell fate decisions.

INTRODUCTION

The study of bacterial lipopolysaccharide (LPS) has provided important insight into the strategies used by the innate immune system to detect infection. Several structurally unrelated LPS receptors exist in mammals, with the best understood being those that promote inflammatory gene expression in macrophages and dendritic cells (DCs). These receptors include the secreted LPS-binding protein (LBP), the GPI-anchored protein CD14, Toll-like Receptor 4 (TLR4), and its associated factor MD-2 (Kieser and Kagan, 2017; Ostuni et al., 2010). Upon bacterial encounters, the activities of LBP and CD14 are coordinated to extract LPS from the bacterial cell wall and deliver this lipid to membrane-associated MD-2 and TLR4. This process leads to TLR4 dimerization and signal transduction, which promotes the expression of genes involved in host defense (Tan and Kagan, 2014). Until recently, it was believed that TLR4 was the sole mediator of cellular responses to LPS (Beutler et al., 2006), with all other LPS receptors merely serving the aforementioned role of ligand delivery. However, recent work revealed LPS responses that act upstream and independent of TLR4 signaling, or in parallel to TLR4 signaling. Upstream of TLR4 signaling is a set of responses mediated by CD14 that induce TLR4 endocytosis (Zanoni et al., 2011). In parallel to TLR4 signaling is the LPS-induced assembly of inflammasomes (Hagar et al., 2013; Kayagaki et al., 2013; Shi et al., 2014). CD14-dependent endocytosis results in the internalization of LPS, CD14, and TLR4 into endosomes, where interferon (IFN)-inducing signaling pathways are activated (Kagan et al., 2008; Zanoni et al., 2011). Inflammasome activation occurs upon detection of LPS in the cytosol by caspase-11 (caspase 4/5 in humans) (Shi et al., 2014). Notably, TLR4-deficient cells retain all these activities. Thus, the collection of cellular responses to LPS can be explained only by the independent activities of multiple LPS receptors (Tan and Kagan, 2014). This view is consistent with the operation of other receptors of the innate immune system that also bind common microbial products (Kieser and Kagan, 2017).

In addition to detecting microbial products, several innate immune receptors detect self-encoded molecules that are found at the sites of tissue damage (Kono and Rock, 2008; Pradeu and Cooper, 2012). These self-encoded ligands are referred to as damage-associated molecular patterns (DAMPs), as opposed to their microbial counterparts, known as pathogen-associated molecular patterns (PAMPs). In contrast to our increasing understanding of how PAMPs are detected, numerous questions remain regarding DAMP detection and signaling. It is generally believed that DAMPs operate as endogenous mimetics of PAMPs and should therefore bind similar receptors and induce similar responses (Bianchi, 2007). In the case of the LPS receptors, the influence of DAMPs on TLR4 signaling is best understood (Schaefer, 2014). Our knowledge of how DAMPs influence other LPS receptors is limited.

oxPAPC is a mixture of oxidized phosphorylcholine derivatives that are commonly associated with dying cells and are considered LPS-like DAMPs (Imai et al., 2008; Shirey et al., 2013). oxPAPC is generated at sites of tissue injury, as these lipids are

produced by the spontaneous oxidation of phosphorylcholine-containing lipids that are present in the plasma membrane of cells (Chang et al., 2004). oxPAPC is an unusual LPS mimic, in that it activates some LPS receptors but not others (Zanoni et al., 2016). For example, oxPAPC does not promote TLR4 responses in murine macrophages or DCs. In contrast, oxPAPC interacts with caspase-11. As such, LPS and oxPAPC promote the caspase-11-dependent assembly of inflammasomes and IL-1β release from DCs. The consequences of LPS and oxPAPC interactions with caspase-11 differ, with LPS inducing IL-1β release and pyroptosis. oxPAPC, in contrast, promotes IL-1β release from living DCs. oxPAPC also forms a complex with caspase-1, independent of caspase-11 (Zanoni et al., 2016), but the consequence of this interaction is unclear. LPS does not interact with caspase-1 (Shi et al., 2014). The ability of oxPAPC to induce IL-1β release without inducing cell death results in a heightened state of DC activation, dubbed "hyperactive" (Zanoni et al., 2016). DCs are the most professional of all antigen-presenting cells (Mellman et al., 1998). As compared to DCs that were activated by TLR ligands alone, hyperactive DCs are superior antigen-presenting cells *in vivo* (Zanoni et al., 2016). In contrast to DCs, macrophages are unable to become hyperactivated by oxPAPC (Zanoni et al., 2016). The features of oxPAPC that permit cell type-specific inflammasome activities are unknown.

In contrast to its ability to hyperactivate DCs that have been pre-exposed to TLR ligands, treatment of naive cells with oxPAPC blocks subsequent responses to LPS via TLR4 (Bochkov et al., 2002; Erridge et al., 2008). Thus, depending on the context, oxPAPC is either an activator or inhibitor of inflammation. It is unknown how oxPAPC elicits these disparate activities.

In this study, we found that CD14 acts as a receptor for oxPAPC. CD14 captured and internalized oxPAPC into endosomes, resulting in a depletion of CD14 from the plasma membrane. This inducible CD14 deficiency at the plasma membrane correlated with decreased responses to subsequent exposures to LPS. CD14 endocytosis also delivered oxPAPC into cells, leading to DC hyperactivation and the release of IL-1 family cytokines. Interestingly, we identified specific lipids within oxPAPC that bound CD14 and promoted macrophage hyperactivation. These lipids induced potentiated inflammatory responses, but not death, in murine models of sepsis. These collective data indicate that CD14 is responsible for the pro- and anti-inflammatory activities of oxPAPC. CD14 can therefore be considered a general regulator of host responses to PAMPs and DAMPs. These observations are consistent with the emerging view of CD14 as a transporter associated with the execution of inflammation (TAXI) (Tan et al., 2015), which captures lipids and receptors as cargo and delivers them to signaling-competent subcellular locations.

RESULTS

oxPAPC Induces a CD14 Deficiency that Diminishes Subsequent Responses to LPS

oxPAPC interferes with LPS interactions with CD14 in cell-free experimental systems, suggesting an interaction between these molecules (Bochkov et al., 2002; Erridge et al., 2008). Within cells, LPS binding by CD14 accelerates the basal endocytosis rate of this receptor and induces the endocytosis of dimerized TLR4 (Tan et al., 2015). To determine whether oxPAPC engages endogenous CD14 or TLR4, we utilized assays that monitor the inducible dimerization or endocytosis of CD14 and TLR4 by flow cytometry. Endocytosis was monitored using antibodies that detect the entire population of CD14 or TLR4 displayed at the cell surface (Sa2-8 and Sa15-21, respectively). Endocytosis results in the loss of surface staining of these proteins (Zanoni et al., 2011). TLR4 dimerization was monitored using a monomer-specific TLR4 antibody (MTS510). Loss of MTS510 surface staining indicates an increase in dimer formation and subsequent endocytosis of these dimers (Tan et al., 2015). Monomer staining at the cell surface indicates the population of receptors that have not interacted with LPS, and therefore are not dimerized. We found that oxPAPC did not induce TLR4 endocytosis, but promoted CD14 endocytosis in immortal bone marrow-derived macrophages (Figures 1A and S1A). oxPAPC had a minimal effect on TLR4 dimerization, with no change in monomer staining observed over the first hour of treatment (Figure S1A). oxPAPC- and LPS-induced CD14 endocytosis proceeded normally in TLR4-deficient cells (Figure 1A). The surface abundance of CD14 is determined by the antagonistic actions of CD14 endocytosis and resynthesis, and endocytosis is most clearly observed under conditions that prevent the latter (Tan et al., 2015). Consequently, the extent of oxPAPC- or LPS-induced CD14 endocytosis was enhanced under conditions where translation was blocked with cycloheximide (Figure S1B). Cycloheximide treatment did not affect LPS-induced TLR4 internalization or dimerization (Figures S1C and S1D). Primary macrophages and bone marrow-derived DCs behaved similar to immortal macrophages, in that oxPAPC promoted CD14 endocytosis but not TLR4 dimerization or endocytosis (Figure 1B). Similar to LPS-induced CD14 endocytosis (Zanoni et al., 2011), oxPAPC-induced CD14 internalization was sensitive to chemical inhibitors of PLCγ (U73122) and Syk (piceatannol) (Figure 1C). These data indicate that oxPAPC and LPS promote CD14 endocytosis by similar mechanisms. In contrast, only LPS promotes TLR4 activities that are associated with its signaling functions, such as dimerization and endocytosis. Consistent with these observations, we found that LPS, but not oxPAPC, induced the phosphorylation of TLR4 signaling regulators, including the Map kinases p38 and ERK1/2 and the transcription factors IRF3, STAT1, and the NF-κB p65 subunit (Figure 1D).

The oxPAPC-induced endocytosis of CD14 (but not TLR4) created a CD14 deficiency at the plasma membrane. This CD14 deficiency may selectively block TLR4 signaling from endosomes, as CD14 is more important for endosomal signaling events than those occurring at the plasma membrane (Moore et al., 2000; Perera et al., 1997; Zanoni et al., 2011). Indeed, oxPAPC-treated cells that were subsequently treated with LPS exhibited defects in TLR4 endocytosis and STAT1 phosphorylation (Figures 1E, 1F, and S2A), as well as the secretion of type I interferon (IFN) and expression of the IFN-stimulated gene *Viperin* (Figure S2B and 1F). All these parameters are classic readouts of TLR4 signaling from endosomes, a process dependent on CD14. LPS-inducible TLR4 dimerization at the plasma membrane was also diminished by oxPAPC pretreatment (Figure 1E), but this inhibition did not correlate with defects in TNFα secretion (Figure S2C). Thus, oxPAPC-treated cells are selectively defective for TLR4 endocytosis and signaling

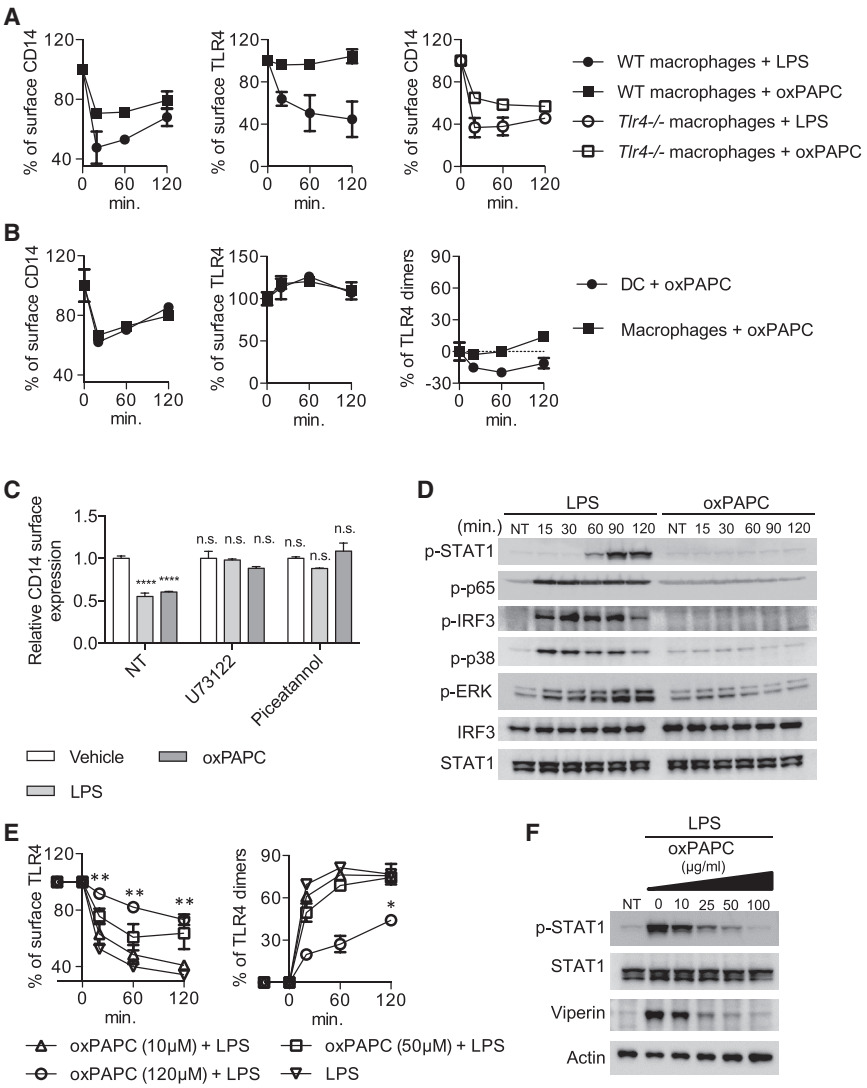

Figure 1. oxPAPC-Induced CD14 Endocytosis Prevents LPS Signaling

(A) Indicated immortal macrophage lines were treated with LPS (1 μg/mL) or oxPAPC (50 μM) for the indicated times. Surface levels of CD14 and TLR4 were measured by flow cytometry. Line graphs represent means and standard deviations of two biological repeats.

(B) Primary DCs and macrophages were treated with oxPAPC (50 μM) for the indicated times. Surface levels of CD14 and TLR4 and TLR4 dimerization were measured by flow cytometry. Line graphs represent means and standard deviations of two independent experiments.

(C) Primary DCs were treated, or not, with LPS (1 μg/mL) or oxPAPC (50 μM) for 15 min in the presence or absence of the PLCγ inhibitor U7322 (5 μM) or the Syk inhibitor Piceatannol (75 μM). Surface levels of CD14 were measured by flow cytometry. Bar graphs represent means and standard deviations of two independent experiments.

(D) Immortal macrophages were treated with LPS or oxPAPC for times indicated. Activation of the type I IFN (p-STAT1 and p-IRF3), NF-κB (p-p65), and MAP kinase (p-p38 and p-ERK1/2) pathways were determined by western analysis.

(E) Immortal macrophages were treated with oxPAPC (at the indicated concentration). Surface levels of TLR4 (left) and TLR4 dimerization (right) were measured by flow cytometry. Line graphs represent means and standard deviations of biological duplicates from one experiment representative of three.

(F) Immortal macrophages were pretreated with indicated concentrations of oxPAPC for 30 min followed by LPS stimulation (10 ng/mL). 4 hr after LPS stimulation, cells were lysed and the activation of the type I IFN pathway were determined by western analysis for p-STAT1 and Viperin.

See also Figure S1.

events from endosomes. The finding that oxPAPC marginally influences signaling events from the plasma membrane eliminates the possibility that, under the conditions used, oxPAPC blocks MD-2 or TLR4 directly, an event that would disrupt all TLR4 signaling events. This ability to dissociate CD14 and TLR4 endocytosis may explain how oxPAPC acts as a TLR4 antagonist.

CD14 Uses the Same Amino Acids to Detect LPS and oxPAPC and Promote Endocytosis

As LPS interactions with CD14 promote endocytosis, it was possible that oxPAPC also binds CD14. We therefore determined whether oxPAPC can interact with CD14 and the amino acids within CD14 that are required for these putative interactions. The LPS-binding domain of CD14 is a large hydrophobic pocket that is comprised of four distinct regions in the N terminus of this protein (Figure 2A; Kim et al., 2005). We have described CD14 alleles that contain mutations in either one region (1R) or two regions (2R), which retained the ability to form a complex with biotinylated LPS (Tan et al., 2015). In contrast, mutations of all four regions (4R) in CD14 abolished LPS-binding activity (Tan et al., 2015). Each of these mutant CD14 alleles encode full-length folded proteins that are transported to the cell surface (Tan et al., 2015). Interestingly, the 4R mutant was also defective for interactions with a biotinylated oxPAPC analog (oxidized PAPE-*N*-biotin, oxPNB, referred to here as "biotin-oxPAPC"), whereas WT, 1R, and 2R CD14 proteins formed a complex with oxPAPC (Figure 2B). We reasoned that if LPS and oxPAPC interact with the same residues in the context of WT CD14, then these lipids should compete for CD14 interactions. In support of this idea, we found that excess unlabeled LPS prevented CD14 interactions with biotin-oxPAPC, with an IC_{50} of 0.5 μM (Figure 2C). Similarly, excess unlabeled oxPAPC prevented CD14 interactions with biotin-LPS, with an IC_{50} of 20 μM (Figure 2C). These findings further suggest direct interactions between CD14 and the lipids

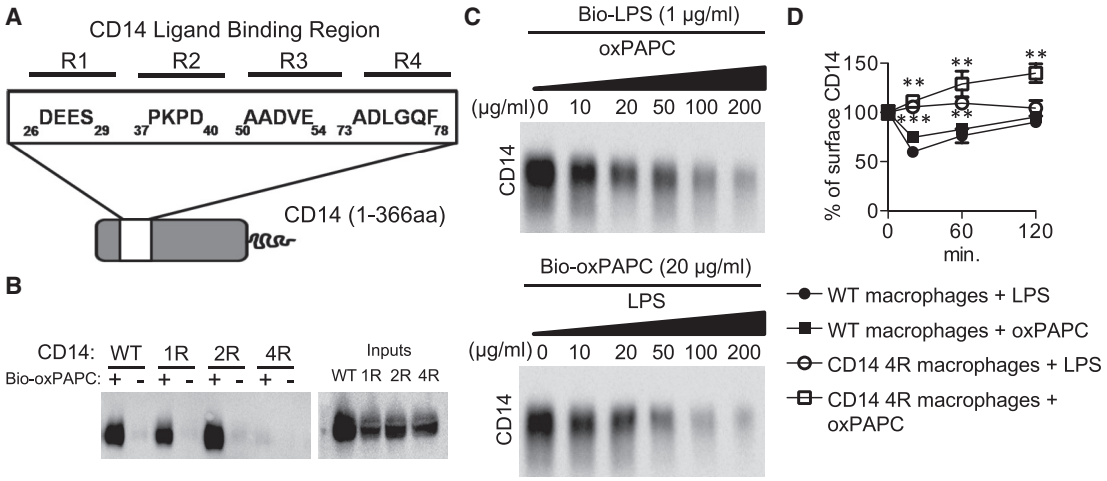

Figure 2. The Same Amino Acids within CD14 Detect oxPAPC and LPS

(A) Schematic of the four regions (R1–R4) used by LPS to induce CD14 internalization.

(B) oxPAPC binding capacity of the CD14 mutants indicated was determined by biotinylated oxPAPC pull down assay. Lysates of 293T cells expressing the indicated CD14 mutants were incubated with biotinylated oxPAPC (10 μg). CD14-oxPAPC complexes were captured using neutravidin beads. The amount of CD14 retained by oxPAPC was determined by western analysis. The CD14 mutant with $_{26}$DEES$_{29}$ mutagenized into $_{26}$AAAA$_{29}$ was designated as CD14 1R. The CD14 mutant with $_{26}$DEES$_{29}$ and $_{37}$PKPD$_{40}$ mutagenized into $_{26}$AAAA$_{29}$ and $_{37}$AAAA$_{40}$ was designated as CD14 2R. The CD14 mutant with $_{26}$DEES$_{29}$, $_{37}$PKPD$_{40}$, $_{52}$DVE$_{54}$, and $_{74}$DLGQ$_{77}$ mutagenized into $_{26}$AAAA$_{29}$, $_{37}$AAAA$_{40}$, $_{52}$AAA$_{54}$, and $_{74}$AAAA$_{77}$ was designated as CD14 4R.

(C) The 4R CD14 mutant is not internalized in response to oxPAPC or LPS treatments. Indicated macrophage lines were treated with LPS (1 μg/mL) or oxPAPC (50 μM) for the times indicated. Surface levels of CD14 were measured by flow cytometry. Line graph represents the average and error bars represent the standard deviation of biological duplicates from one representative experiment of three. Statistical significance of WT versus CD14 4R cells is shown for each treatment.

(D) Lysates of 293T cells expressing CD14 were pretreated with indicated concentrations of oxPAPC (top) or LPS (bottom) for 30 min and then incubated with biotinylated LPS (1 μg/mL) (top) or biotinylated oxPAPC (20 μg/mL) (bottom). CD14-LPS (top) or CD14-oxPAPC (bottom) complexes were captured using neutravidin beads. The amounts of CD14 retained by biotinylated LPS (top) or biotinylated oxPAPC (bottom) were determined by western analysis. Representative blots from at least two independent experiments were shown.

See also Figure S2.

examined and provide evidence that CD14 may bind preferentially to LPS. Finally, when stably introduced into CD14-deficient immortal macrophages, the 4R CD14 mutant was not internalized in response to LPS or oxPAPC treatments (Figure 2D). We therefore conclude that CD14 is an oxPAPC receptor, and the same amino acids within CD14 mediate interactions with oxPAPC and LPS. These interactions are important to promote CD14 endocytosis. Interestingly, using the same procedures to monitor CD14 interactions, we found that oxPAPC also formed a complex with MD-2 (Figure S2D). As CD14 acts upstream of MD-2, this interaction cannot explain the actions of oxPAPC on CD14 binding or endocytosis. It is possible that in cells that naturally lack CD14, oxPAPC may bind directly to MD-2 and prevent LPS interactions with the same. But in phagocytes, CD14 must be considered the likely functional target of oxPAPC.

oxPAPC Promotes CD14-Dependent DC Hyperactivation

In addition to promoting CD14 endocytosis, oxPAPC induces DC hyperactivation, which is defined by the ability of these cells to release IL-1β while retaining viability (Zanoni et al., 2016). To determine the relationship between the activities of oxPAPC to promote CD14 endocytosis and promote DC hyperactivation, we examined the requirement of CD14 for oxPAPC-induced IL-1β release. DCs were primed with LPS for 3 hr, which is sufficient time to re-populate the plasma membrane with newly synthesized CD14 (Tan et al., 2015), and stimulated with oxPAPC. Interestingly, we found that CD14 was required for oxPAPC-induced IL-1β release, as LPS-primed CD14-deficient DCs released minimal IL-1β in response to oxPAPC (Figure 3A). Similar results were obtained when the TLR2 ligand Pam3CSK (P3C) was used to prime cells (Figure 3B). TNFα secretion was not affected by the loss of CD14 in any of the conditions tested (Figures 3A and 3B). To corroborate these findings, we examined IL-18, another cytokine that is released via the actions of inflammasomes. Whereas LPS-primed DCs released IL-18 in response to oxPAPC treatment, CD14-deficient DCs were unable to do so (Figure 3C). In contrast, when the inflammasome activator ATP was used as a stimulus, IL-18 release was unaffected by CD14 deficiency (Figure 3C). We also observed a requirement for caspase-11 in promoting IL-18 release in response to oxPAPC (Figure 3C), as shown previously for IL-1β (Zanoni et al., 2016).

Similar results were obtained when we stimulated DCs that were first isolated from the spleens of WT, CD14-deficient, or caspase-11-deficient mice. LPS-stimulated splenic DCs upregulated surface abundance of the co-stimulatory molecule CD86, in the presence or absence of oxPAPC (Figures S3A and S3B). LPS-primed cells released IL-1β after oxPAPC treatment, by a process dependent on CD14 and caspase-11 (Figure 3D). TNFα secretion was unaffected by CD14 or caspase-11 deficiencies in splenic DCs, and ATP stimulations of LPS-primed cells induced IL-1β release independently of CD14 and caspase-11 (Figure 3D).

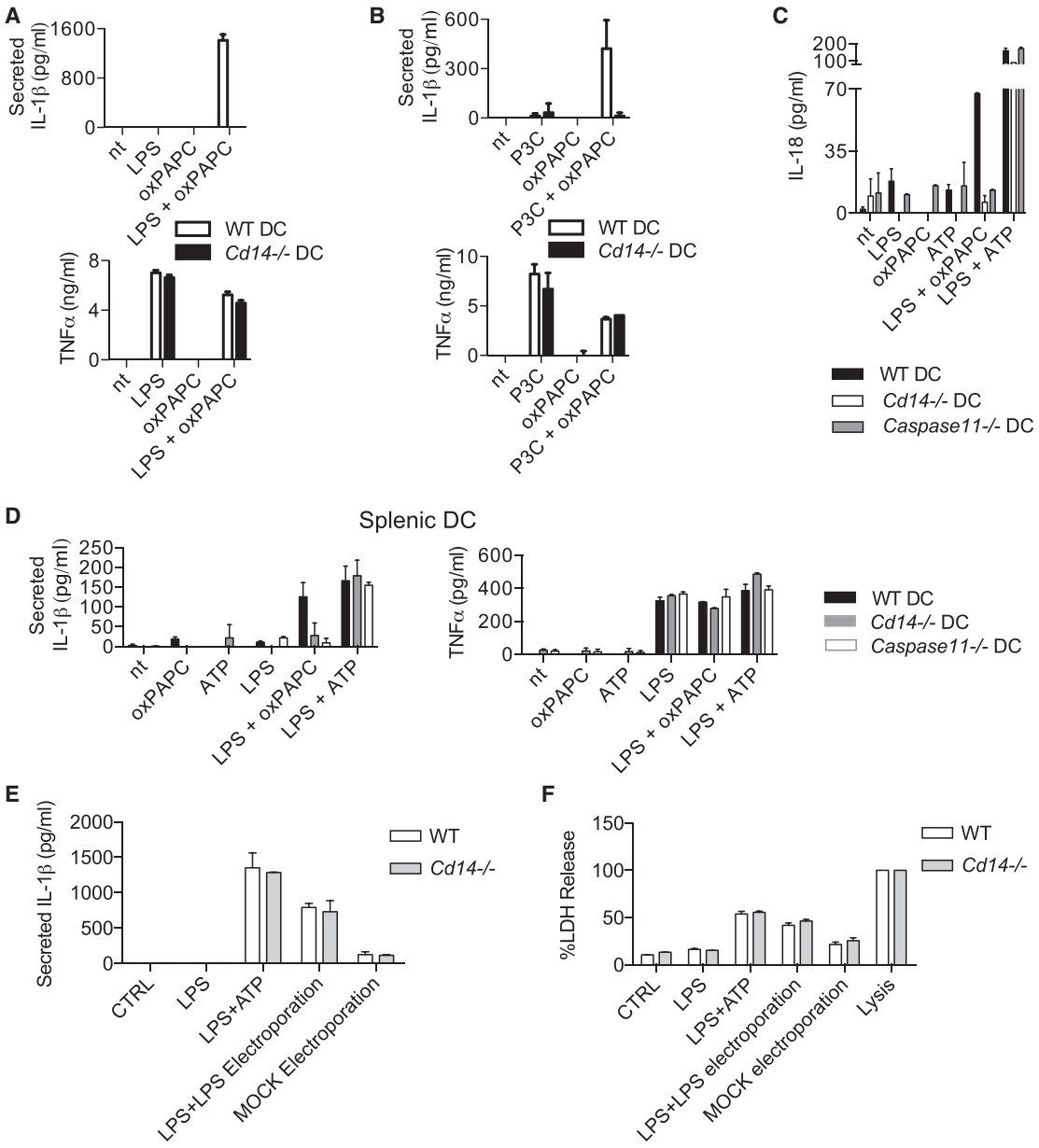

Figure 3. CD14 Promotes Caspase-11-Mediated IL-1β and IL-18 Release from DCs

(A and B) WT DCs and CD14-deficient DCs were treated with LPS (1 μg/mL), Pam3CSK (P3C) (1 μg/mL), or oxPAPC (120 μM) or were primed with LPS or P3C for 3 hr and then treated with oxPAPC. 18 hr after LPS (A) or P3C (B) administration, IL-1β and TNFα secretion was measured by ELISA. Means and standard deviations of two independent experiments are shown.

(B) Spleen-derived WT DCs, CD14-deficient DCs, and Caspase-11-deficient DCs were treated with LPS (1 μg/mL), ATP (1.5 mM), or oxPAPC (120 μM) or were primed with LPS for 3 hr and then treated with oxPAPC or ATP. 18 hr after LPS administration, IL-1β and TNFα secretion was measured by ELISA. Means and standard deviations of two replicates of one representative experiment of three are shown.

(C) WT DCs, CD14-deficient DCs, and Caspase-11-deficient DCs were treated with LPS (1 μg/mL), oxPAPC (120 μM), or ATP (1 mM) or were primed with LPS for 3 hr and then treated with oxPAPC or ATP. IL-18 was measured by ELISA in the supernatant 18 hr later.

(D) Spleen-derived WT DCs, CD14-deficient DCs, and Caspase-11-deficient DCs were treated with LPS (1 μg/mL), ATP (1.5 mM), or oxPAPC (120 μM) or were primed with LPS for 3 hr and then treated with oxPAPC or ATP. 18 hr after LPS administration, IL-1β (left) and TNFα (right) secretion was measured by ELISA. Means and standard deviations of two replicates of one representative experiment of three are shown.

(E and F) WT and CD14-deficient DCs were either primed with LPS (1 μg/mL) for 3 hr and then treated with ATP (1 mM) or were electroporated with LPS (1 μg/mL) or MOCK electroporated. IL-1 (E) and LDH (F) release was monitored 18 hr later.

See also Figure S3.

While oxPAPC and ATP promote inflammasome-dependent cytokine release, the major distinction between these DAMPs is that oxPAPC promotes DC hyperactivation, whereas ATP promotes pyroptosis. CD14 must therefore be considered a selective regulator of DC hyperactivation.

CD14 Does Not Regulate the Priming Phase of Inflammasome Activation

To understand the function of CD14 in DC hyperactivation, we considered the possibility that this receptor regulated cell priming. However, three lines of evidence invalidated this possibility. First, the dose of LPS used (1 μg/mL) bypassed the requirement of CD14 for TLR4-induced cytokine expression, as assessed by analysis of *Il1b* transcripts and secretion of TNFα (Figures S4A and 3A). Second, P3C-primed DCs also required CD14 for oxPAPC-induced IL-1β release (Figure 3B), even though P3C primes cells via TLR2, independent of CD14 (Figure S4A). Finally, ATP-induced IL-1β and IL-18 release was unaffected by CD14 deficiency (Figures 3C and 3D), an observation that would not be possible if a priming defect existed.

In other experimental settings, type I IFNs promote caspase-11 expression and/or activation (Broz et al., 2012; Case et al., 2013; Rathinam et al., 2012). Since CD14 promotes IFN production in response to LPS treatment, as observed by its requirement for *Viperin* expression (Figure S4A), we determined whether recombinant IFNβ (rIFNβ) could bypass the need of CD14 for oxPAPC-induced IL-1β release. However, rIFNβ was unable to restore the ability of oxPAPC to elicit IL-1β release from CD14-deficient cells (Figure S4B). In addition, oxPAPC elicited IL-1β release from DCs that were primed with P3C (Figure 3B), which did not produce functional type I IFNs, as indicated by a lack of *Viperin* expression (Figure S4A). These experiments therefore indicate that IFN-mediated priming is not necessary for oxPAPC-induced inflammasome activation.

The expression of *Caspase-1*, *Caspase-11*, *Nlrp3*, and *Asc* mRNAs was largely unaffected by the lack of CD14 in unstimulated or LPS- or P3C-stimulated DCs (Figure S4C). However, minor differences in *Caspase-1* and *Caspase-11* expression were observed in LPS-treated cells (Figure S4C). We reasoned that if these differences have functional consequences, then a defect in LPS-induced inflammasome activities should be evident in CD14-deficient DCs. LPS-primed WT and CD14-deficient DCs were electroporated with LPS to examine Caspase-11- and Caspase-1-dependent responses. Notably, WT and CD14-deficient cells responded equally to electroporation of LPS, in terms of IL-1β release (Figure 3E) and pyroptosis induction, as measured by lactate dehydrogenase (LDH) release (Figure 3F). These findings indicate that the amount of Caspase-1 and Caspase-11 present in CD14-deficient cells is sufficient to elicit inflammasome-dependent responses. Collectively, these data indicate that CD14 is not required for cell priming. CD14 may therefore have a direct role in promoting inflammasome-dependent IL-1β release in response to oxPAPC.

CD14 Transports oxPAPC into the Cell to Promote DC Hyperactivation

To determine how CD14 promotes inflammasome activities, we considered the endocytosis-promoting activities of this receptor. Since oxPAPC binds to and promotes CD14 endocytosis, we reasoned that CD14 transports oxPAPC into the cell to promote IL-1β release. CD14 may therefore be important to capture oxPAPC from the extracellular space. Consistent with this idea, a fluorescently labeled component of oxPAPC (TopFluor-PGPE) strongly labeled the surface of DCs, as assessed by live-cell confocal microscopy (Figure 4A). This labeled lipid was also observed in endosomal vesicles (Figure 4A). In contrast, CD14-deficient DCs displayed minimal staining of the plasma membrane by the labeled oxPAPC component (Figure 4A). This defect in the capture of extracellular molecules by CD14-deficient cells was specific, as comparable dextran labeling was observed in WT and CD14-deficient cells (Figure 4A). Thus, CD14 captures oxPAPC and delivers this lipid into the cell.

We reasoned that if the primary function of CD14 is to deliver oxPAPC into the cell, then it should be possible to bypass the requirement of CD14 by delivering oxPAPC into the cell via alternative means. The transfection reagent DOTAP is a useful tool to deliver inflammatory stimuli directly to endosomes and the cytosol (Honda et al., 2005). WT and CD14-deficient DCs were therefore primed with P3C and then exposed to DOTAP, in complex with LPS or oxPAPC. As expected, LPS was unable to induce IL-1β release when administered to the extracellular media, but DOTAP-mediated delivery of LPS promoted IL-1β release from WT and CD14-deficient DCs (Figure 4B). Interestingly, altering the entry route of oxPAPC into the cells by DOTAP yielded similar results. Whereas extracellular oxPAPC could not elicit IL-1β release from primed CD14-deficient DCs, oxPAPC in complex with DOTAP elicited IL-1β release from CD14-deficient cells, in a Caspase-dependent manner (Figure 4B). Cell-associated pro-IL-1β was largely unaffected by these treatments (Figure 4C). An alternative delivery mechanism can therefore bypass the requirement of CD14 for oxPAPC-induced IL-1β release. These collective data highlight an important role of CD14 in the capture and delivery of oxPAPC into the cell, where inflammasome-mediated DC hyperactivation can occur.

Meta-analysis Reveals Essential and Possibly Redundant Regulators of DC Hyperactivation

To compare the importance of CD14 to that of other regulators of oxPAPC-induced DC hyperactivation, we performed a meta-analysis of multiple genotypes of bone marrow-derived DCs. We plotted the percent of IL-1β release that remained in genetically deficient cells, as compared to WT cells, across 4–16 experiments (depending on genotype) (Figure 5A). From this analysis, Asc, Nlrp3, and Caspase-1 emerged as most critical for IL-1β release, with virtually no residual IL-1β release occurring in cells lacking the genes encoding these proteins (Figure 5A). These findings are consistent with the functions of these proteins as core components of most inflammasomes. CD14 and Caspase-11 were also validated as important regulators of IL-1β release, but cells lacking these proteins exhibited residual (10%–30%) cytokine release (Figure 5A). The residual IL-1β release associated with Caspase-11 deficiency may be explained by the ability to oxPAPC to bind independently to Caspase-11 and Caspase-1 (Zanoni et al., 2016), perhaps forming distinct complexes that are important for inflammasome assembly. This possibility requires further investigation. The residual cytokine release detected in CD14-deficient DCs, however, is unexplained. To verify the residual IL-1β release associated

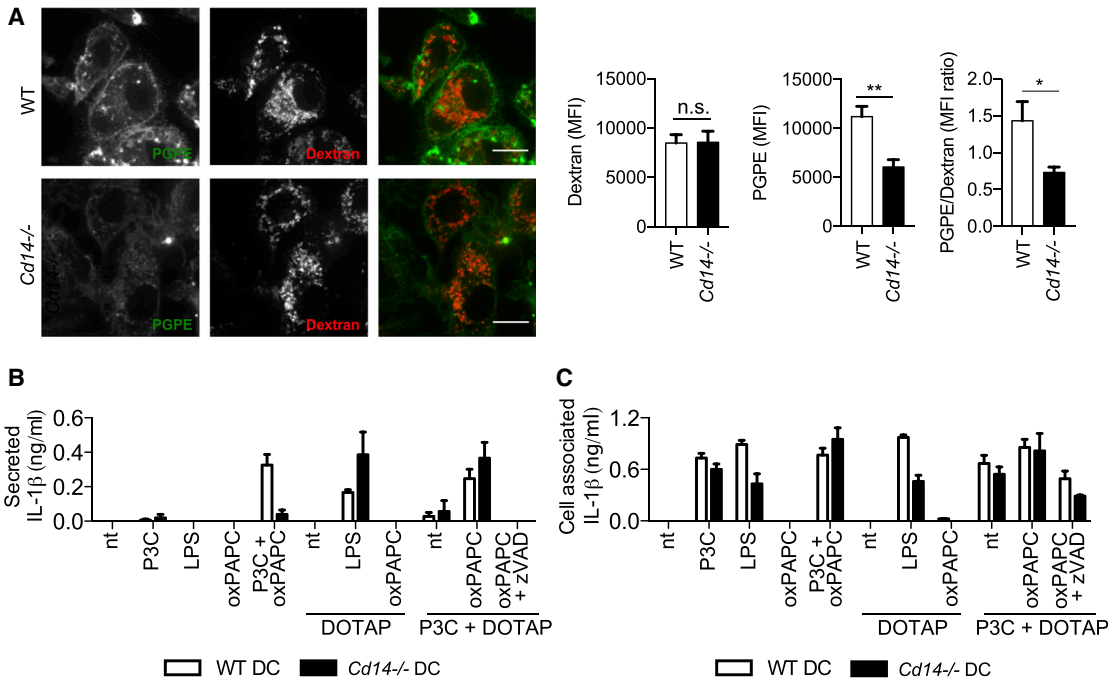

Figure 4. CD14 Transports oxPAPC into the Cell to Promote Inflammasome Activities

(A) WT DCs and CD14-deficient DCs were treated with TopFluor-PGPE (5 μg/mL, green) and Alexa568-labeled dextran (200 μg/mL, red) for 1 hr. Cell were imaged by confocal microscopy. Fluorescent images and quantification are representative of three independent experiments. Scale bar: 10 μm.

(B and C) WT DCs and CD14-deficient DCs were treated with LPS (1 μg/mL), P3C (1 μg/mL), or oxPAPC (120 μM) or were primed with P3C for 3 hr and then treated with oxPAPC. As indicated, LPS or oxPAPC were complexed with DOTAP before addition to the cell culture. Where indicated, cells where treated with the pan-Caspase inhibitor zVAD 30 min before addition of the DOTAP/oxPAPC complex to the culture. 18 hr after stimuli administration, secreted (B) or cell-associated (C) IL-1β were measured by ELISA. Means and standard deviations of two independent experiments are shown.

See also Figure S4.

with CD14 deficiency, we examined the presence of this cytokine in the supernatants of oxPAPC-stimulated DCs by western analysis. Cells lacking CD14 exhibited diminished, albeit incomplete, loss of the processed p17 fragment of IL-1β from the extracellular media (Figure 5B). It is possible that CD14-deficient cells may permit some low-level capture of oxPAPC from the extracellular space by macropinocytosis, with functional consequences. Indeed, WT and CD14-deficient DCs displayed comparable macropinocytosis activities, as assessed by the capture of extracellular fluorescent dextrans (Figures 4A and 5C). Thus, while it is possible that redundant means of oxPAPC delivery into the cell exist, CD14 is the dominant receptor responsible for inflammasome-dependent DC hyperactivation.

Specific oxPAPC Components Hyperactivate Macrophages and Promote Inflammation *In Vivo*

Most known inducers of inflammasome responses display activity in DCs and macrophages (Latz et al., 2013). However, DCs are specifically hyperactivated by oxPAPC; macrophages are not (Zanoni et al., 2016). To better understand the ability of oxPAPC to induce cell type-specific inflammasome activities, we sought to define the bioactive components of oxPAPC. Our previous work identified the oxPAPC components PGPC (1-palmitoyl-2-glutaryl-*sn*-glycero-3-phosphocholine) and POVPC (1-palmitoyl-2-(5′-oxo-valeroyl)-*sn*-glycero-3-phosphocholine) as molecules that elicit IL-1β release from LPS-primed DCs (Zanoni et al., 2016). We found that these lipids were minor components of oxPAPC, individually comprising fewer than 10% of the total lipids present in parental oxPAPC mixture (Figures S5A and S5B). Interestingly, PGPC and POVPC induced the release of IL-1β from LPS-primed macrophages and DCs, whereas oxPAPC displayed this activity only in DCs (Figures 6A and 6B). TNFα secretion in response to all stimulations that included LPS was observed in both cell types (Figures 6A and 6B). The cleaved p17 fragment of IL-1β was detected in the extracellular media of LPS-primed DCs and macrophages treated with PGPC and POVPC (Figures 6C and 6D), which argues strongly for an inflammasome-dependent event. In contrast, cleaved IL-1β was detected in the extracellular media only of LPS-primed DCs, not macrophages, stimulated with oxPAPC (Figures 6C and 6D).

To determine whether PGPC and POVPC induced macrophage hyperactivation, several assays for cell viability were performed. We first performed a visual examination of cell monolayers 24 hr after various stimulations. These studies demonstrated that LPS-primed and ATP-treated WT or CD14-deficient macrophages became rounded and swollen (Figure S6A). These cells detached from the tissue culture plate, as a single wash with PBS removed almost all cells (Figure S6B), and ATP-treated macrophages that were primed with LPS released LDH (Figure S6C). These features are hallmarks of pyroptosis. Interestingly, LPS-primed cells that were exposed to oxPAPC or its components maintained cell morphology and adherence and

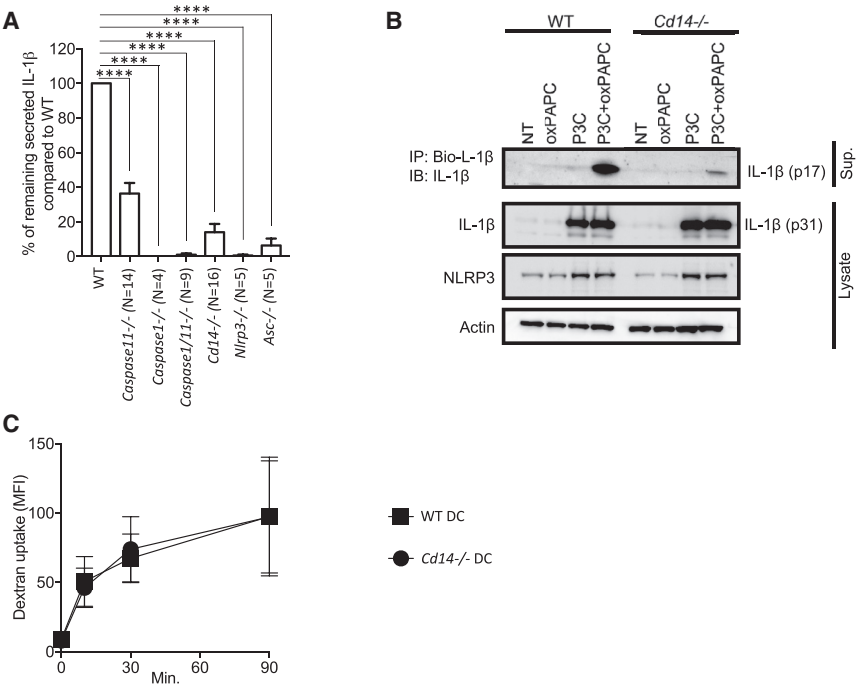

Figure 5. Essential and Possibly Redundant Regulators of oxPAPC-Dependent Inflammasome Activities in DCs

(A) DCs derived from the indicated backgrounds were primed with LPS (1 μg/mL) and stimulated with oxPAPC (120 μM). Their capacity to secrete IL-1β was compared with WT DCs stimulated in the same manner. Percentages of remaining IL-1β compared to WT DCs are shown. N: number of independent measurement analyzed for each genetic background. Means and standard errors are shown.

(B) WT DCs and CD14-deficient DCs were primed or not with P3C and activated or not with oxPAPC (120 μM). Supernatant (Sup) of non-treated (NT) or P3C-primed (P3C) cells were incubated with a biotinylated antibody directed against IL-1β (Bio-αIL-1β). IL-1β associated with the biotinylated antibody was captured by streptavidin beads and revealed by western analysis. Cell lysates (Lysate) were probed with the indicated antibodies. Shown is a representative blot out of three independent experiments.

(C) FITC-Dextran uptake by WT DCs and CD14-deficient DCs was measured over time by cytofluorimetry. Line graphs represent the average and error bars represent the standard deviation of six independent experiments.

See also Figure S5.

did not release LDH (Figures S6A–6C). In addition, macrophages exposed to PGPC or POVPC released increasing amounts of IL-1β over 48 hr—an attribute that is consistent with cell viability (Figure 6B). DCs behaved similarly in the presence of oxPAPC or its component lipids over 48 hr (Figures 6A and 6B). These data therefore support the idea that PGPC and POVPC can induce IL-1β release from living macrophages and DCs.

To determine whether the abilities of PGPC and POVPC to induce IL-1β release was a process similar to that induced by oxPAPC in DCs, we determined whether these lipids interact with CD14. This possibility was examined indirectly, by determining whether PGPC or POVPC compete with LPS for access to CD14. We found that excess unlabeled PGPC or POVPC prevented CD14 interactions with biotin-LPS (Figure 6E), with an IC_{50} of 9.2 μM and 16.8 μM, respectively. As oxPAPC and LPS interactions with CD14 promote endocytosis (Figure 1), we examined whether PGPC and POVPC induce CD14 endocytosis. PGPC and POVPC induced the rapid endocytosis of CD14 in macrophages and DCs (Figure 6F). These collective studies support the conclusion that PGPC and POVPC are ligands for CD14.

To determine the function of CD14 in PGPC- and POVPC-induced IL-1β release, we examined IL-1β release from WT and CD14-deficient macrophages and DCs. LPS-primed macrophages and DCs required CD14 in order to release IL-1β in response to PGPC and POVPC treatments (Figures 6A and 6B). We also noted that residual IL-1β release was observed in the absence of CD14 in both cell types, which is an observation similar to what we observed with oxPAPC in DCs (Figures 5A and 5B). TNFα secretion and cell survival were minimally affected by the absence of CD14 (Figures 6A, 6B, and S6A–S6C). Similar to oxPAPC in DCs, IL-1β secretion in response to POVPC or PGPC was dependent on NLRP3 and Caspase-1/11 in LPS-primed macrophages (Figure 6G).

For these studies, it was critical to eliminate the role of CD14 in cell priming by LPS. Thus, we sought to partially mimic LPS priming by treating cells with a CD14-independent stimulus, P3C, and rIFNβ. WT macrophages that were primed in this manner released IL-1β into the extracellular space upon treatment with PGPC and POVPC, and this process was largely dependent on CD14 (Figures S7A and S7B). In contrast, CD14 was not required for ATP-induced release of IL-1β from similarly primed cells (Figures S7C and S7D). Notably, PGPC and POVPC induced the continuous release of IL-1β from primed macrophages, as evidenced by the increase in detectable IL-1β in the extracellular media 96 hr after treatment (Figure S7A). In contrast, and as expected, ATP stimulation of primed cells resulted in a short-term release of IL-1β, with no increase of this cytokine between 24 and 96 hr after treatment (Figures S7C and S7D). Moreover, visual examination of cells stimulated for 24 hr revealed that POVPC- and PGPC-treated macrophages retained morphology (Figures S7E and S7F). These cells released low levels of LDH over this time frame (Figures S7E and S7F). At this low level, LDH release is not associated with other morphological features of pyroptosis, so the significance of this observation is unclear. ATP treatments, in contrast, were lethal to the cell population, as visual inspection revealed substantial cell rounding and robust LDH release after 24 hr (Figures S7E and S7F). Taken together, these data establish that specific components within oxPAPC can engage CD14 to promote IL-1β release from living macrophages.

While our *in vitro* studies have delineated the abilities of oxPAPC and its components to hyperactivate phagocytes and not induce pyroptosis, the effects of these different phagocyte activation states *in vivo* are unclear. At present, we are limited in our ability to directly assess pyroptosis or cell hyperactivation *in vivo*. However, a strong functional correlation exists between

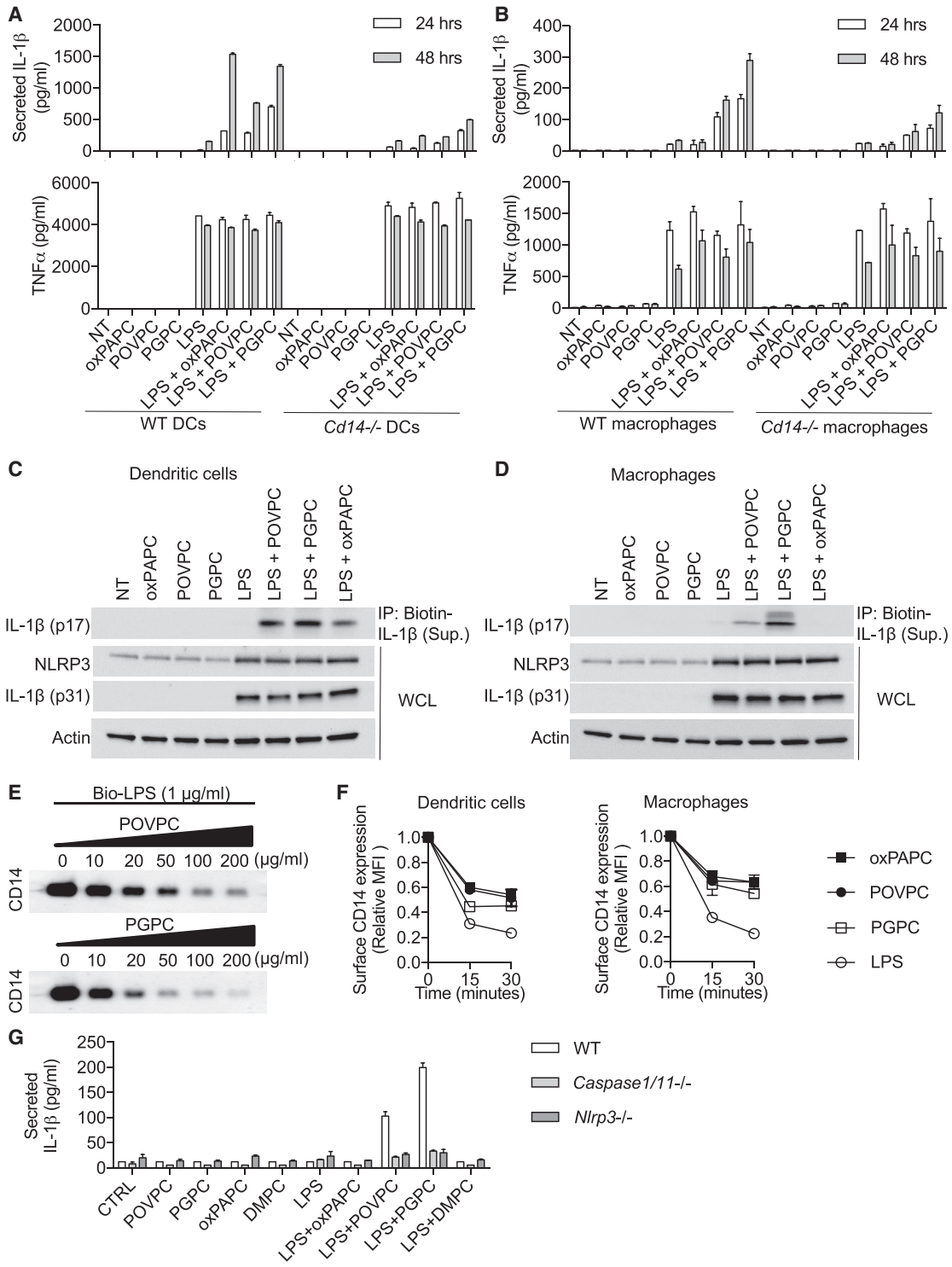

Figure 6. CD14 Promotes DC and Macrophage Hyperactivation in Response to oxPAPC Components

(A and B) WT or CD14-deficient DCs (A) or macrophages (B) were activated (or not) for 3 hr with LPS and stimulated, or not, with oxPAPC (120 μM), POVPC (120 μM), PGPC (120 μM). 18 hr after LPS administration, IL-1β (top) and TNFα (bottom) secretion was measured by ELISA. Means and standard deviations of two replicates of one representative experiment of three are shown.

(C and D) WT or CD14-deficient DCs (A) or macrophages (B) were activated (or not) for 3 hr with LPS and stimulated, or not, with oxPAPC (120 μM), POVPC (120 μM), PGPC (120 μM). 18 hr after LPS administration, processed IL-1β in the tissue culture supernatants from DCs (C) or macrophages (D) was captured by a biotinylated IL-1β antibody followed by western analysis. Expression levels of cell associated pro-IL-1 β and NLRP3 in DCs (C) or macrophages (D) were determined by western analysis.

(legend continued on next page)

conditions that promote pyroptosis *in vitro* and those that induce lethal sepsis *in vivo* (Hagar et al., 2013; Kayagaki et al., 2013). Indeed, the ability of LPS to kill mice depends on its ability to induce pyroptosis (Hagar et al., 2013; Kayagaki et al., 2013). As oxPAPC and its components promote IL-1β release but not pyroptosis *in vitro*, we expected that a similar correlation would exist *in vivo*, and oxPAPC would induce inflammation but not lethality. To address this possibility, mice were primed (or not) by intraperitoneal injection of LPS for 5 hr and were subsequently challenged by injection with a second dose of LPS, oxPAPC, PGPC, or vehicle (Figure 7A). Mice were monitored for viability, and serum cytokines were measured 2 hr and 30 hr after challenge. LPS-primed mice that were challenged with vehicle retained viability throughout the experiment and displayed no or low levels of serum IL-1β, IL-6, and TNFα (Figures 7B–7G). In contrast, LPS-primed mice that received a second dose of LPS displayed increased amounts of serum IL-1β, IL-6, and TNFα within 2 hr of challenge (Figures 7B–7D). These results are consistent with prior findings (Li et al., 1995). LPS-primed mice that were challenged with oxPAPC or PGPC for 2 hr also displayed increased amounts of IL-1β, IL-6, and TNFα, as compared to vehicle-challenged mice (Figures 7B–7D), although each challenge yielded different amounts of each cytokine. Comparable amounts of IL-6 were found in the serum of LPS-, oxPAPC-, and PGPC-injected mice 2 hr after challenge, whereas each lipid induced different amounts of IL-1β or TNFα release (Figures 7B–7D). Interestingly, whereas LPS-primed mice that were challenged with LPS all died within 30 hr, no loss of animal viability was observed in LPS-primed mice that were challenged with oxPAPC or PGPC (Figure 7E). 30 hr after challenge, oxPAPC- and PGPC-treated mice still displayed increased serum cytokines, although each challenge resulted in different cytokines being detected (Figures 7F and 7G). These collective results demonstrate that conditions that promote pyroptosis *in vitro* (double LPS treatments) lead to lethal sepsis *in vivo*, whereas conditions that promote phagocyte hyperactivation *in vitro* (LPS and oxPAPC treatments) lead to inflammation (but not death) *in vivo*. These findings support the idea that phagocyte hyperactivation is a bona fide cell activation state that can be observed in multiple experimental settings.

DISCUSSION

In this study, we explored how oxPAPC can have the opposing activities of (1) interfering with TLR4 signaling to prevent inflammatory responses and (2) hyperactivating cells to promote inflammation. Our studies demonstrate that CD14 is a central regulator of both activities.

We found that CD14 bound oxPAPC and captured these lipids from the extracellular space. Upon capture, CD14 and oxPAPC were delivered into the cell via endocytosis. oxPAPC-induced CD14 endocytosis diminished the abundance of CD14 at the plasma membrane, creating an inducible CD14 deficiency that rendered cells poorly responsive to subsequent encounters with LPS. Interestingly, we observed a similar behavior of the anti-inflammatory LPS derived from *Rhodobacter spheroides* (Tan et al., 2015), which is the prototype lipid of the commercialized TLR4 antagonist Eritoran. When administered to naive cells, oxPAPC and *R. spheroides* LPS promoted CD14 endocytosis, but not TLR4 endocytosis, thus creating a functional CD14 deficiency. It therefore appears that a common means by which TLR4 antagonists operate is by the inducible removal of CD14 from the plasma membrane.

Our prior work highlighted how CD14 functions to transport LPS and TLR4 to signaling-competent regions of the cells, thus revealing this protein as a TAXI (Tan et al., 2015). The findings reported in this study are consistent with this idea and expand the function of CD14 beyond its role as a TAXI for LPS and TLR4. Rather, CD14 must now be considered a general TAXI for inflammatory lipids derived from the host or microbe. Furthermore, the endocytosis-promoting activities of CD14 must now be considered in a context of broader significance than simply regulating TLR4 activities. In the case of oxPAPC, for example, CD14 captured and delivered this DAMP into the cell to promote IL-1β release. CD14 therefore represents the earliest-acting regulator of DC hyperactivation, serving as an oxPAPC receptor. These conclusions, however, do not rule out the possibility that other oxPAPC receptors operate to capture this lipid from the extracellular media, with functionally important consequences. Indeed, other receptors may explain the residual oxPAPC-induced IL-1β release that is observed in CD14-deficient cells.

That CD14 acts as a functional receptor of oxPAPC is notable, because there are several examples of extracellular molecules that promote inflammasome assembly and IL-1β release. However, it is unclear how many of these molecules are captured by cells. One thoroughly characterized means by which extracellular molecules are delivered into the cell to promote inflammasome activities is via the actions of bacterial pore-forming toxins or secretion systems. Our finding that CD14 is an oxPAPC receptor that is required for DC hyperactivation therefore provides insight into the earliest stages of the inflammatory response. It remains unclear how oxPAPC is delivered from endosomes into the cytosol. We note several other immunological processes involve such a transport event, such as the transport of extracellular antigens to the MHC class I machinery (Cruz et al., 2017),

(E) Lysates of 293T cells expressing CD14 were pretreated with indicated concentrations of POVPC or PGPC for 30 min and then incubated with biotinylated LPS (1 μg). CD14-LPS complex was captured using neutravidin beads. The amount of CD14 retained by LPS in the presence of POVPC or PGPC was determined by western analysis. Representative blots from at least two independent experiments were shown.
(F) WT DCs or macrophages were treated with oxPAPC (120 μM), POVPC (120 μM), and PGPC (120 μM) for indicated time periods. Surface levels of CD14 from DCs or macrophages were measured by flow cytometry. Line graphs with standard deviations represent the average of duplicate readings from one representative experiment out of three.
(G) WT, Caspase1/11 double-deficient, and NLRP3-deficient macrophages were treated with LPS or not for 3 hr, and then treated, or not, with oxPAPC (120 μM), POVPC (120 μM), PGPC (120 μM), and DMPC (120 μM). IL-1β secretion was measured by ELISA. Means and standard deviations of two replicates of one representative experiment out of three are shown.
See also Figure S6.

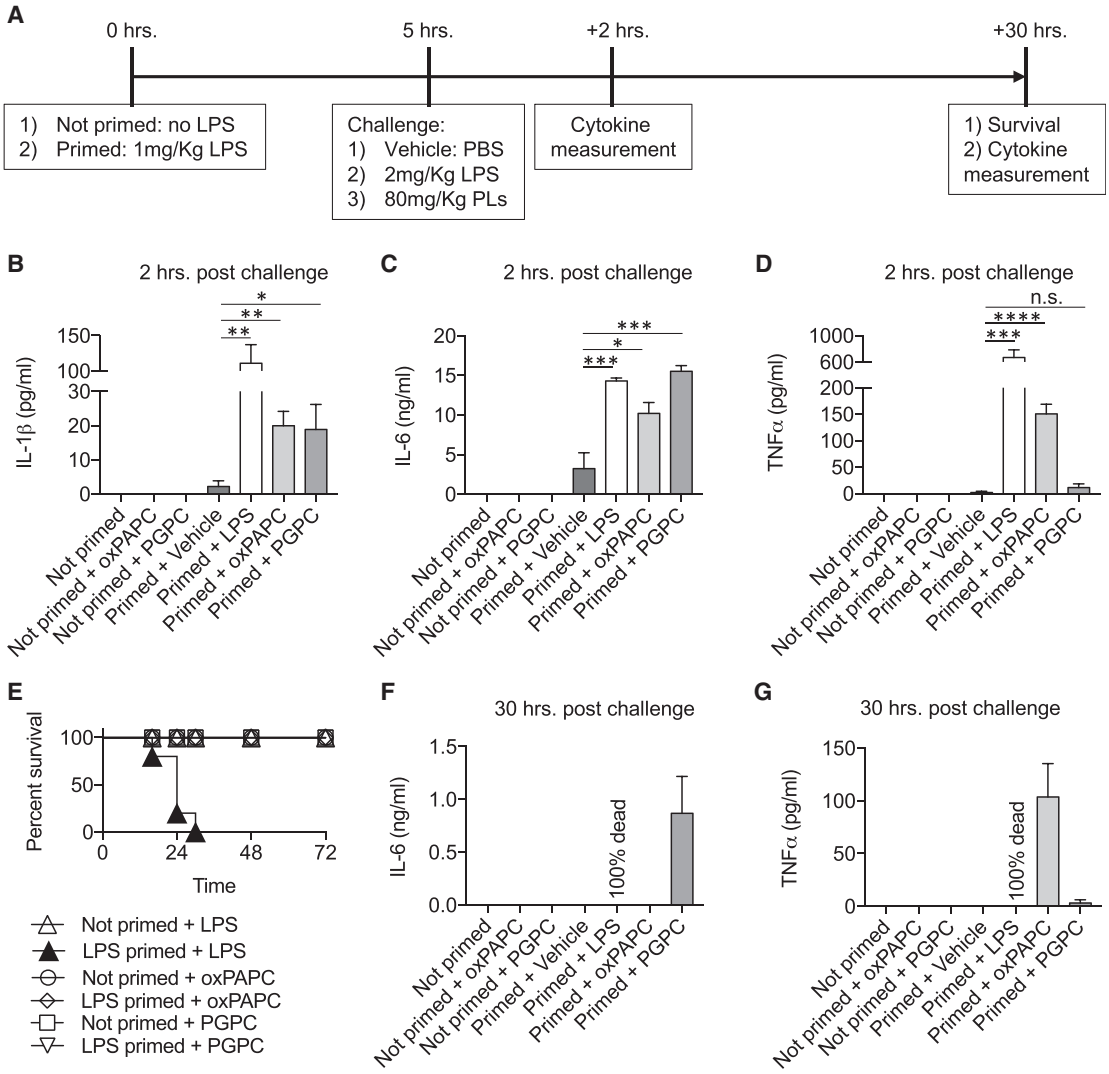

Figure 7. Conditions that Hyperactivate Phagocytes Induce Inflammatory Sepsis in Mice, but Not Death

(A) Schematic representation of the *in vivo* experimental setting. PLs, phospholipids.

(B–D) ELISA of serum cytokines from mice treated as in (A) 2 hr after challenge.

(E) Survival curves of mice treated as in (A).

(F and G) ELISA of serum cytokines from mice treated as in (A) 30 hr after challenge.

and the delivery of peptidoglycan fragments to NOD1 and NOD2 in the cytosol (Philpott et al., 2014). Our knowledge of how endosomal molecules are transported to the cytosol remains limited.

The identification of specific lipids within oxPAPC that hyperactivated macrophages is also notable, as the heterogenous oxPAPC mixture can hyperactivate only DCs (Zanoni et al., 2016). We found that, similar to oxPAPC, PGPC and POVPC competed with LPS for access to CD14 *in vitro*, promoted CD14 endocytosis, and promoted IL-1β release from living macrophages, by a CD14- and inflammasome-dependent process. It is unclear why PGPC and POVPC were able to hyperactivate macrophages only in isolation, and not when present within the heterogenous oxPAPC mixture. This observation may be explained by the fact that macrophages contain more degradative endo-lysosomes than DCs (Delamarre et al., 2005). As PGPC and POVPC represent fewer than 10% of the total lipids within oxPAPC (Figure S5), it is possible that high concentrations of these lipids are necessary to allow any bioactive lipids to escape macrophage endosomes and promote inflammasome-dependent phagocyte hyperactivation.

A notable feature of hyperactive cells is their unusual ability to maintain viability while releasing IL-1 family cytokines. Evidence supporting this conclusion is several-fold, as treatment of cells with oxPAPC or its individual components promoted the release of IL-1, but not LDH. These cells also maintained plasma membrane integrity and maintained mitochondrial activity (Zanoni et al., 2016). Furthermore, as shown in this study, these cells maintained morphology and the ability to attach to tissue culture plates and release IL-1 continuously over the course of several days. In contrast, pyroptotic cells (which have been treated

with ATP or transfected with LPS) released LDH and lost plasma membrane integrity, morphology, adhesiveness, and mitochondrial activity. These cells were able to release IL-1β only over a short time frame (hours). Thus, inflammasomes can induce two opposing cell fate decisions—pyroptosis and cell hyperactivation.

Is it possible that non-pyroptotic death pathways contribute to the long-term IL-1β release that typifies the hyperactive state of phagocytes? At the population level, the answer must be yes. It is formally possible that some of the released IL-1β results from apoptotic programs that are induced 24–96 hr after stimulation. However, these putative programs cannot explain the finding that POVPC and PGPC promote inflammasome-dependent events that cleave pro-IL-1β, in the absence of any notable features of pyroptosis. Live single cell imaging may be necessary to explore these possibilities fully.

In murine models of inflammatory sepsis, the opposing cell fate decisions of pyroptosis and hyperactivation have profound consequences, as conditions that promote pyroptosis *in vitro* lead to lethal inflammatory sepsis *in vivo*. In contrast, conditions that promote cell hyperactivation *in vitro* lead to inflammation but not lethality *in vivo*. These findings are consistent with the idea that inflammatory cytokine production must be coupled with pyroptosis in order to induce lethality in response to LPS injections of mice. These findings further demonstrate that the state of cell hyperactivation exists *in vitro* and *in vivo*. It is also worth noting that oxPAPC is not unique in its ability to hyperactivate cells. Recent work has identified the *N*-acetyl glucosamine fragment of bacterial peptidoglycan as being able to elicit IL-1 release from living macrophages (Wolf et al., 2016), and LPS is sufficient to induce the same response in human and pig monocytes (Gaidt et al., 2016). Thus, select DAMPs and PAMPs have the ability to hyperactivate phagocytes. These new findings, coupled with our demonstration that hyperactivating stimuli (LPS and oxPAPC treatments) are superior inducers of adaptive immunity than activating stimuli (LPS alone) (Zanoni et al., 2016) support the importance of understanding this newly defined aspect of phagocyte biology.

The collection of information available allows us to propose a working model of how oxPAPC and its component lipids operate *in vivo*. We propose that oxPAPC is an inhibitor of TLR4 signaling, but only when cells are pre-exposed to these lipids—before they encounter LPS. oxPAPC exposures in the absence of LPS may mimic environments associated with sterile tissue injury. Under these conditions, CD14 endocytosis after interactions with oxPAPC may render cells less responsive to any TLR4-activating DAMPs that are present in the damaged tissue. This response limits the risk of autoimmunity. Under conditions of oxPAPC and LPS co-exposure, TLR4 signaling is not blocked. Rather, oxPAPC enhances inflammatory activities by inducing an inflammasome-dependent state of cell hyperactivation. We speculate that conditions of oxPAPC and LPS co-exposure may mimic the environment associated with virulent pathogenic encounters, where tissue damage and PAMPs are abundant. Under these conditions, a hyperactive cell state may be important to fight virulent pathogens. This work therefore provides a mandate to consider the role of CD14 and other regulators of phagocyte hyperactivation in controlling the activities of inflammatory lipids in the host and microbial world.

STAR★METHODS

Detailed methods are provided in the online version of this paper and include the following:

- KEY RESOURCES TABLE
- CONTACT FOR REAGENT AND RESOURCE SHARING
- EXPERIMENTAL MODEL AND SUBJECT DETAILS
  - Cell culture
- METHOD DETAILS
  - Gene expression analysis and ELISA
  - *In vitro* protein-lipid interactions
  - Western analysis
  - Flow cytometry
  - LPS Electroporation
  - Microscopy imaging of cell morphology and live cell imaging
  - *In vivo* challenges
- QUANTIFICATION AND STATISTICAL ANALYSIS

SUPPLEMENTAL INFORMATION

Supplemental Information includes seven figures and can be found with this article online at https://doi.org/10.1016/j.immuni.2017.09.010.

AUTHOR CONTRIBUTIONS

I.Z., Y.T., and M.D. performed all research. J.R.S. synthesized custom lipids. J.C.K. supervised all research. All authors discussed results and commented on the manuscript.

ACKNOWLEDGMENTS

We thank members of the Kagan and Zanoni labs for helpful discussions. We thank L.R. Marek especially, for inspiring a critical stage of this project. J.C.K. is supported by NIH grants AI093589, AI116550, and P30 DK34854. J.C.K. holds an Investigators in the Pathogenesis of Infectious Disease Award from the Burroughs Wellcome Fund. I.Z. is supported by NIH grants 1R01AI121066-01A1, 1R01DK115217, and P30 DK034854, Harvard Medical School Milton Found, CCFA Senior Research Awards (412708), and the Cariplo Foundation (2014-0859). J.R.S. is supported by NIH grant 1R15HL121770-01A1. Y.T. is supported by a postdoctoral fellowship of the Jane Coffin Childs Fund (the Merck Fellow).

Received: November 11, 2016
Revised: June 20, 2017
Accepted: September 20, 2017
Published: October 17, 2017

REFERENCES

Beutler, B., Jiang, Z., Georgel, P., Crozat, K., Croker, B., Rutschmann, S., Du, X., and Hoebe, K. (2006). Genetic analysis of host resistance: Toll-like receptor signaling and immunity at large. Annu. Rev. Immunol. *24*, 353–389.

Bianchi, M.E. (2007). DAMPs, PAMPs and alarmins: all we need to know about danger. J. Leukoc. Biol. *81*, 1–5.

Bochkov, V.N., Kadl, A., Huber, J., Gruber, F., Binder, B.R., and Leitinger, N. (2002). Protective role of phospholipid oxidation products in endotoxin-induced tissue damage. Nature *419*, 77–81.

Broz, P., Ruby, T., Belhocine, K., Bouley, D.M., Kayagaki, N., Dixit, V.M., and Monack, D.M. (2012). Caspase-11 increases susceptibility to *Salmonella* infection in the absence of caspase-1. Nature *490*, 288–291.

Case, C.L., Kohler, L.J., Lima, J.B., Strowig, T., de Zoete, M.R., Flavell, R.A., Zamboni, D.S., and Roy, C.R. (2013). Caspase-11 stimulates rapid

flagellin-independent pyroptosis in response to *Legionella pneumophila*. Proc. Natl. Acad. Sci. USA *110*, 1851–1856.

Chang, M.K., Binder, C.J., Miller, Y.I., Subbanagounder, G., Silverman, G.J., Berliner, J.A., and Witztum, J.L. (2004). Apoptotic cells with oxidation-specific epitopes are immunogenic and proinflammatory. J. Exp. Med. *200*, 1359–1370.

Cruz, F.M., Colbert, J.D., Merino, E., Kriegsman, B.A., and Rock, K.L. (2017). The biology and underlying mechanisms of cross-presentation of exogenous antigens on MHC-I molecules. Annu. Rev. Immunol. *35*, 149–176.

Delamarre, L., Pack, M., Chang, H., Mellman, I., and Trombetta, E.S. (2005). Differential lysosomal proteolysis in antigen-presenting cells determines antigen fate. Science *307*, 1630–1634.

Erridge, C., Kennedy, S., Spickett, C.M., and Webb, D.J. (2008). Oxidized phospholipid inhibition of toll-like receptor (TLR) signaling is restricted to TLR2 and TLR4: roles for CD14, LPS-binding protein, and MD2 as targets for specificity of inhibition. J. Biol. Chem. *283*, 24748–24759.

Gaidt, M.M., Ebert, T.S., Chauhan, D., Schmidt, T., Schmid-Burgk, J.L., Rapino, F., Robertson, A.A., Cooper, M.A., Graf, T., and Hornung, V. (2016). Human monocytes engage an alternative inflammasome pathway. Immunity *44*, 833–846.

Hagar, J.A., Powell, D.A., Aachoui, Y., Ernst, R.K., and Miao, E.A. (2013). Cytoplasmic LPS activates caspase-11: implications in TLR4-independent endotoxic shock. Science *341*, 1250–1253.

Honda, K., Ohba, Y., Yanai, H., Negishi, H., Mizutani, T., Takaoka, A., Taya, C., and Taniguchi, T. (2005). Spatiotemporal regulation of MyD88-IRF-7 signalling for robust type-I interferon induction. Nature *434*, 1035–1040.

Imai, Y., Kuba, K., Neely, G.G., Yaghubian-Malhami, R., Perkmann, T., van Loo, G., Ermolaeva, M., Veldhuizen, R., Leung, Y.H., Wang, H., et al. (2008). Identification of oxidative stress and Toll-like receptor 4 signaling as a key pathway of acute lung injury. Cell *133*, 235–249.

Kagan, J.C., Su, T., Horng, T., Chow, A., Akira, S., and Medzhitov, R. (2008). TRAM couples endocytosis of Toll-like receptor 4 to the induction of interferon-beta. Nat. Immunol. *9*, 361–368.

Kayagaki, N., Wong, M.T., Stowe, I.B., Ramani, S.R., Gonzalez, L.C., Akashi-Takamura, S., Miyake, K., Zhang, J., Lee, W.P., Muszyński, A., et al. (2013). Noncanonical inflammasome activation by intracellular LPS independent of TLR4. Science *341*, 1246–1249.

Kieser, K.J., and Kagan, J.C. (2017). Multi-receptor detection of individual bacterial products by the innate immune system. Nat. Rev. Immunol. *17*, 376–390.

Kim, J.I., Lee, C.J., Jin, M.S., Lee, C.H., Paik, S.G., Lee, H., and Lee, J.O. (2005). Crystal structure of CD14 and its implications for lipopolysaccharide signaling. J. Biol. Chem. *280*, 11347–11351.

Kono, H., and Rock, K.L. (2008). How dying cells alert the immune system to danger. Nat. Rev. Immunol. *8*, 279–289.

Latz, E., Xiao, T.S., and Stutz, A. (2013). Activation and regulation of the inflammasomes. Nat. Rev. Immunol. *13*, 397–411.

Li, P., Allen, H., Banerjee, S., Franklin, S., Herzog, L., Johnston, C., McDowell, J., Paskind, M., Rodman, L., Salfeld, J., et al. (1995). Mice deficient in IL-1 beta-converting enzyme are defective in production of mature IL-1 beta and resistant to endotoxic shock. Cell *80*, 401–411.

Mellman, I., Turley, S.J., and Steinman, R.M. (1998). Antigen processing for amateurs and professionals. Trends Cell Biol. *8*, 231–237.

Moore, K.J., Andersson, L.P., Ingalls, R.R., Monks, B.G., Li, R., Arnaout, M.A., Golenbock, D.T., and Freeman, M.W. (2000). Divergent response to LPS and bacteria in CD14-deficient murine macrophages. J. Immunol. *165*, 4272–4280.

Ostuni, R., Zanoni, I., and Granucci, F. (2010). Deciphering the complexity of Toll-like receptor signaling. Cell. Mol. Life Sci. *67*, 4109–4134.

Perera, P.Y., Vogel, S.N., Detore, G.R., Haziot, A., and Goyert, S.M. (1997). CD14-dependent and CD14-independent signaling pathways in murine macrophages from normal and CD14 knockout mice stimulated with lipopolysaccharide or taxol. J. Immunol. *158*, 4422–4429.

Philpott, D.J., Sorbara, M.T., Robertson, S.J., Croitoru, K., and Girardin, S.E. (2014). NOD proteins: regulators of inflammation in health and disease. Nat. Rev. Immunol. *14*, 9–23.

Pradeu, T., and Cooper, E.L. (2012). The danger theory: 20 years later. Front. Immunol. *3*, 287.

Rathinam, V.A., Vanaja, S.K., Waggoner, L., Sokolovska, A., Becker, C., Stuart, L.M., Leong, J.M., and Fitzgerald, K.A. (2012). TRIF licenses caspase-11-dependent NLRP3 inflammasome activation by gram-negative bacteria. Cell *150*, 606–619.

Schaefer, L. (2014). Complexity of danger: the diverse nature of damage-associated molecular patterns. J. Biol. Chem. *289*, 35237–35245.

Shi, J., Zhao, Y., Wang, Y., Gao, W., Ding, J., Li, P., Hu, L., and Shao, F. (2014). Inflammatory caspases are innate immune receptors for intracellular LPS. Nature *514*, 187–192.

Shirey, K.A., Lai, W., Scott, A.J., Lipsky, M., Mistry, P., Pletneva, L.M., Karp, C.L., McAlees, J., Gioannini, T.L., Weiss, J., et al. (2013). The TLR4 antagonist Eritoran protects mice from lethal influenza infection. Nature *497*, 498–502.

Tan, Y., and Kagan, J.C. (2014). A cross-disciplinary perspective on the innate immune responses to bacterial lipopolysaccharide. Mol. Cell *54*, 212–223.

Tan, Y., Zanoni, I., Cullen, T.W., Goodman, A.L., and Kagan, J.C. (2015). Mechanisms of Toll-like receptor 4 endocytosis reveal a common immune-evasion strategy used by pathogenic and commensal bacteria. Immunity *43*, 909–922.

Wolf, A.J., Reyes, C.N., Liang, W., Becker, C., Shimada, K., Wheeler, M.L., Cho, H.C., Popescu, N.I., Coggeshall, K.M., Arditi, M., and Underhill, D.M. (2016). Hexokinase is an innate immune receptor for the detection of bacterial peptidoglycan. Cell *166*, 624–636.

Zanoni, I., Ostuni, R., Marek, L.R., Barresi, S., Barbalat, R., Barton, G.M., Granucci, F., and Kagan, J.C. (2011). CD14 controls the LPS-induced endocytosis of Toll-like receptor 4. Cell *147*, 868–880.

Zanoni, I., Ostuni, R., Barresi, S., Di Gioia, M., Broggi, A., Costa, B., Marzi, R., and Granucci, F. (2012). CD14 and NFAT mediate lipopolysaccharide-induced skin edema formation in mice. J. Clin. Invest. *122*, 1747–1757.

Zanoni, I., Tan, Y., Di Gioia, M., Broggi, A., Ruan, J., Shi, J., Donado, C.A., Shao, F., Wu, H., Springstead, J.R., and Kagan, J.C. (2016). An endogenous caspase-11 ligand elicits interleukin-1 release from living dendritic cells. Science *352*, 1232–1236.

STAR★METHODS

KEY RESOURCES TABLE

REAGENT or RESOURCE	SOURCE	IDENTIFIER
Antibodies		
Mouse monoclonal Anti-β-Actin	Sigma-Aldrich	A5441; RRID: AB_476744
Rabbit monoclonal Anti-phospho Stat-1	Cell Signaling Technology	9167; RRID: AB_561284
Rabbit monoclonal anti-phospho IRF3 (4D4G)	Cell Signaling Technology	4947s; RRID: AB_823547
Rabbit monoclonal anti-phospho p65 (93H1)	Cell Signaling Technology	3033S; RRID: AB_331284
Mouse monoclonal anti-Phospho p38	BD Biosciences	612288; RRID: AB_399605
Mouse monoclonal anti-Phospho ERK1/2	Cell Signaling Technology	9106s; RRID: AB_331768
Mouse monoclonal anti-Viperin	BioLegend	Custom made 91736
Rabbit polyclonal Anti-IL-1β	GeneTex	GTX74034; RRID: AB_378141
Mouse monoclonal Anti-NLRP3	Adipogen	AG-20B-0014-C100
Biotinylated Anti-IL-1β	R&D Systems	BAF401
PE Anti-TLR4 (clone: Sa15-21)	BioLegend	145404; RRID: AB_2561874
PE/Cy7 Anti-TLR4/MD2 complex (clone: MTS510)	BioLegend	117610; RRID: AB_2044020
FITC Anti-CD14 (clone: Sa2-8)	Thermo Scientific	11-0141-82; RRID: AB_464949
APC Anti-CD14 (clone: Sa2-8)	Thermo Scientific	17-0141-82
Chemicals and Recombinant Proteins		
E. coli LPS Serotype O111:B4 S-form	Enzo Life Sciences	ALX-581-012-L002
oxPAPC	InvivoGen	tlrl-oxp1
Pam3CSK4	InvivoGen	tlrl-pms
POVPC	Cayman chemical	N° 10031
PGPC	Cayman chemical	N° 10044
DMPC	Avanti Lipids Polar	850345
Oxidized PAPE-N-biotin	James R. Springstead Laboratory	N/A
Biotinylated LPS	InvivoGen	tlrl-3blps
TopFluor-PGPE	Avanti Lipids Polar	810402
Alexa568-Dextran	Thermo Scientific	D22912
FITC-Dextran	Sigma-Aldrich	FD10S
DOTAP	Sigma-Aldrich	11202375001 ROCHE
U-73122	Sigma-Aldrich	U6756
Piceatannol	Sigma-Aldrich	P0453
zVADfmk	Sigma-Aldrich	V116-2MG
Recombinant mouse IFN-β protein	R&D Systems	8234-MB-010
Critical Commercial Assays		
Mouse IL-1β ELISA Kit	Thermo Scientific	88-7013-22
Mouse TNFα ELISA Kit	Thermo Scientific	88-7324-88
Mouse IL-18 ELISA Kit	Thermo Scientific	BMS618-3
LDH Cytotoxicity Assay Kit	Thermo Scientific	88953
Deposited Data		
CD14 mutants	Jonathan Kagan Laboratory	PMID: 26546281
Experimental Models: Organisms/Strains		
Mouse: C57BL/6J	The Jackson Laboratory	000664
Mouse: B6.129S4-Cd14tm1Frm/J	The Jackson Laboratory	003726
Mouse: B6.129S4(D2)-Casp4tm1Yuan/J	The Jackson Laboratory	024698
Mouse: B6N.129S2-Casp1tm1Flv/J	The Jackson Laboratory	016621
Mouse: *Nlrp3*$^{-/-}$	Tiffany Horng Laboratory	N/A

(*Continued on next page*)

Continued		
REAGENT or RESOURCE	SOURCE	IDENTIFIER
Mouse: *Asc*$^{-/-}$	Tiffany Horng Laboratory	N/A
Mouse: *Caspase-1*$^{-/-}$	Thirumala-Devi Kanneganti Laboratory	N/A
Experimental Models: Cell lines		
Immortalized bone marrow-derived macrophages (iBMDMs)	Jonathan Kagan Laboratory	N/A.
Bone marrow-derived dendritic cells	Jonathan Kagan Laboratory	N/A
Bone marrow-derived macrophages	Jonathan Kagan Laboratory	N/A
Splenic dendritic cells	Jonathan Kagan Laboratory	N/A
Cd14−/− iBMDMs expressing CD14 WT and mutant alleles	Jonathan Kagan Laboratory	PMID: 26546281
TaqMan probes		
Viperin	Thermo Scientific	Mm00491265_m1
Caspase-1	Thermo Scientific	Mm00438023_m1
Caspase-11	Thermo Scientific	Mm00432307_m1
Nlrp3	Thermo Scientific	Mm00840904_m1
Asc	Thermo Scientific	Mm00445747_g1
TBP	Thermo Scientific	Mm00446971_m1
Software and Algorithms		
ImageJ	NIH	https://imagej.nih.gov/ij/

CONTACT FOR REAGENT AND RESOURCE SHARING

Further information and requests for resources and reagents should be directed to and will be fulfilled by the Lead Contact, Jonathan C. Kagan (jonathan.kagan@childrens.harvard.edu).

EXPERIMENTAL MODEL AND SUBJECT DETAILS

Cell culture

DCs were differentiated from bone marrow in IMDM (GIBCO), 10% B16-GM-CSF derived supernatant, 2 μM 2-mercaptoethanol and 10% FBS and used after 6 days of culture. DC purity was assessed by flow cytometry and was usually higher than 90%. Macrophages were differentiated from bone marrow in DMEM (GIBCO), 30% L929 supernatant, and 10% FBS. Immortal macrophages were cultured in DMEM supplemented with 10% L929 supernatant and 10% FBS. Splenic DCs were purified as described previously (Zanoni et al., 2012). Prior to stimulations, cultured cells were washed and re-plated in DMEM supplemented with 10% FBS at a concentration of $1x10^6$ cells/ml in a final volume of 100μl. For experiments using pan-caspase inhibitor, cells were treated with zVADfmk (20μM) 30 min before inflammasome stimuli addition. Transfection with DOTAP was performed following the manufacturer instructions. Briefly, 375ng of DOTAP were added to 5μg of LPS or 10μg of oxPAPC in a final volume of 10μl of DMEM without FBS. 30 min later, the DOTAP complexes were added to the culture.

METHOD DETAILS

Gene expression analysis and ELISA

RNA was isolated from cell cultures using Qiashedder (QIAGEN) and GeneJET RNA Purification Kit (Life Technologies). Purified RNA was analyzed for gene expression on a CFX384 real time cycler (Bio-rad) using TaqMan RNA-to-CT 1-Step Kit (Applied Biosystems) with gene-specific probes.

ELISA were performed to measure secreted cytokines. Briefly, supernatants were collected, clarified by centrifugation and stored at −20°C. Cell associated cytokines were measured as follows: 96-well plates were centrifuged and supernatant was discarded. 250μl of PBS were added to each well. Cells were frozen and thawed two times at −80°C and then stored at −20°C for further analysis.

In vitro protein-lipid interactions

oxPAPC binding capacity of the indicated CD14 mutants was determined by the biotinylated oxPAPC pull down assay. Lysates of 293T cells expressing the indicated CD14 mutants were incubated with biotinylated oxPAPC (10 μg), the CD14-oxPAPC complex was then captured using streptavidin beads. The amount of CD14 retained by oxPAPC was determined by western analysis. Detailed information about the generation of CD14 mutants is described elsewhere (Tan et al., 2015). Briefly, a full length CD14 cDNA was

subjected to site-directed mutagenesis. The CD14 mutant with $_{26}$DEES$_{29}$ mutagenized into $_{26}$AAAA$_{29}$ was designated as CD14 1R. The CD14 mutant with $_{26}$DEES$_{29}$ and $_{37}$PKPD$_{40}$ mutagenized into $_{26}$AAAA$_{29}$ and $_{37}$AAAA$_{40}$ was designated as CD14 2R. The CD14 mutant with $_{26}$DEES$_{29}$, $_{37}$PKPD$_{40}$, $_{52}$DVE$_{54}$ and $_{74}$DLGQ$_{77}$ mutagenized into $_{26}$AAAA$_{29}$, $_{37}$AAAA$_{40}$, $_{52}$AAA$_{54}$ and $_{74}$AAAA$_{77}$ was designated as CD14 4R.

Western analysis

For western analysis, immortal macrophages (5x10^6) were stimulated with ligands for the times indicated, and lysed in 700 μL of lysis buffer containing 1% NP-40, 50mM Tris-HCl (pH 7.4), 150mM NaCl. Protease inhibitors and phosphatase inhibitors were added just prior to cell lysis. Immunoblotting was performed using standard techniques.

For measurement of processed IL-1β released into the extracellular space, cell culture supernatants from DCs were collected. IL-1β was captured with a biotinylated IL-1β antibody, and subsequently isolated via streptavidin beads for 2 hr on a nutator at 4°C. After washing, samples were eluted in SDS loading buffer and separated by SDS-PAGE. Captured IL-1β was detected by western analysis. NLRP3 and Pro-IL-1β in the cell lysates were determined on a separate blot. Actin was probed as loading control.

Flow cytometry

Immortal macrophages, primary bone marrow derived macrophages and DCs or splenic DCs (0.5x10^6) of the indicated genotypes were treated with *E.coli* LPS and/or oxPAPC for the indicated time points at 37°C. Cells were then washed with 1 mL cold PBS and stained for appropriate antibodies on ice for 20 to 30 min. 2% mouse serum or rat serum were used as the blocking reagent to reduce non-specific binding of the antibodies. The stained cells were then washed with 1ml cold PBS and resuspended in 200 μL PBS. Staining of the surface receptors was analyzed with BD FACSCanto II. The mean fluorescence intensity (MFI) of CD14 and TLR4 from unstimulated or stimulated cells were recorded. The percentage of surface receptor staining at indicated time points, which is the ratio of the MFI values measured from the stimulated cells to those measured from the unstimulated cells, was plotted to reflect the efficiency of receptor endocytosis. For measuring the extent of TLR4/MD-2 dimerization, the percentage of TLR4/MD2 dimer was calculated by 100%-the percentage of TLR4/MD-2 monomer. The percentage of the TLR4/MD-2 monomer was determined by the ratio of the MFI values (obtained from MTS510 antibody staining) of the stimulated cells to those of the unstimulated cells.

LPS Electroporation

For LPS electroporation into LPS-primed WT and CD14 macrophages, the Neon transfection system (Life Technologies) was used with 10^6 primed-cells plus 1 μg LPS per chamber condition with the following program (Voltage: 1400 V; Width: 20 ms; Pulses: 2 pulses). Electroporated cells were immediately plated into pre-warmed antibiotic-free complete RPMI and then cultured for 24 hours.

Microscopy imaging of cell morphology and live cell imaging

To determine cell morphology after inflammasome stimulation, macrophages were seeded in 12-well plates (0.5 × 10^6 /ml per well) and were subjected to treatments indicated. For static image capture, a Nikon Eclipse TS100 microscope was used with 20 x or 40 x magnification. Images were processed with the ''NIS-Elements F'' software. Representative images were chosen from at least three randomly chosen fields from one experiment out of two independent experiments.

For live cell imaging, DCs seeded into a 35 mm glass bottom dish (Ibidi) were incubated with 5 μg/ml TopFluor-PGPE (Avanti Polar Lipids, inc.) and 200 μg/ml Alexa568-labeled dextran (Thermo Scientific) for one hour. Images were acquired with a Zeiss Axiovert 200M inverted confocal microscope and the level of single cell fluorescent intensity for the two channels was analyzed using ImageJ software (NIH).

In vivo challenges

Female mice aged 8 weeks were primed via intraperitoneal (i.p.) injection with 1 mg/kg *E. coli* LPS or vehicle control for 5 hours. Mice were then challenged via i.p. injection with the stimuli indicated. The mice were monitored for 30 hours for survival and serum blood samples were collected at 2 hours and 30 hours post-challenge for cytokine analysis. All animal procedures were approved by IACUC.

QUANTIFICATION AND STATISTICAL ANALYSIS

Statistical significance for experiments with more than two groups was tested with One way Anova and Tukey multiple comparison tests were performed. Two Way ANOVA with Tukey multiple comparison test was used to analyze kinetic experiments. When comparisons between only two variables were made, unpaired two tailed t test was used to assess statistical significance. Adjusted p values were calculated with Prism7 (Graphpad) or with Excel. Asterisk coding, also indicated in figure legends, is depicted as follows: *$p \leq 0.05$; **$p \leq 0.01$; ***$p \leq 0{,}001$; ****$p \leq 0{,}0001$.